Gondwana Research 16 (2009) 264–271

Contents lists available at ScienceDirect

Gondwana Research

journal homepage: www.elsevier.com/locate/gr

A Re–Os study of molybdenites from the Lanjiagou Mo deposit of North China Craton and its geological significance

Chunming Han [a,*], Wenjiao Xiao [a], Guochun Zhao [b], Min Sun [b], Wenjun Qu [c], Andao Du [c]

[a] State Key laboratory of Lithospheric Evolution, Institute of Geology and Geophysics, Chinese Academy of Sciences, Beijing, 100029, China
[b] Department of Earth Sciences, The University of Hong Kong, Pokfulam Road, Hong Kong, China
[c] National Research Center of Geoanalysis, Beijing, 100037, China

ARTICLE INFO

Article history:
Received 15 October 2008
Received in revised form 15 December 2008
Accepted 4 January 2009
Available online 7 January 2009

Keywords:
Re–Os study
Mo deposit
Lanjiagou
North China Craton

ABSTRACT

The Lanjiagou Mo deposit is located in the eastern part of the North China Craton. Rhenium and osmium isotopes in molybdenites from the Lanjiagou porphyry Mo deposit have been used to determine the timing of mineralization. Molybdenite was analyzed mainly from granite porphyry, which is characterized by moderate to strong silicification. Rhenium concentrations in molybdenite samples are between 33 and 48 μg/g. Analysis of eleven molybdenite samples yields an isochron age of 181.6±6.5 Ma (2σ). Based on the geological history and spatio-temporal distribution of the granitoids, it is proposed that the Mo deposits in the eastern part of the North China Craton were related to the subduction of the Paleo-Pacific plate during Jurassic time.

1. Introduction

The North China Craton bears the most important molybdenum metallogenic province in China, which consists of the Yanshan–Liaoning molybdenum ore belt on the northern margin and the Eastern Qinling molybdenum ore belt on the southern margin (Huang et al., 1996). Located on the northern margin of the North China Craton (NCC), the Yanshan–Liaoning molybdenum ore belt is one of the centralized areas of important molybdenum deposits, as well as one of the major molybdenum producers in China. The time and space of these deposits are associated with intermediate-acid granites. The molybdenum (copper) deposits are usually distributed along the endo- or exo-contact zones of granite porphyries, and belong to porphyry-type (e.g. Lanjiagou), porphyry–skarn-type (e.g. Xiaojiayingzi, Dawan and Xiaochigou) and skarn-type (e.g. Yangjiazhangzi and Shouwangfen) ore deposits (Table 1; Fig. 2).

The Lanjiagou Mo deposit is located in the eastern part of the NCC (Figs. 1 and 2). Regionally and tectonically, it occurs in the eastern part of the Mesozoic Yanshan fold belt. It was discovered by the Liaoning Bureau of Geology and General Corporation of Non-ferrous Metallurgic Metals in the 1950s. Presently, the mining exploration is still being performed by the local government. The reserve of molybdenum metal in the deposit has been estimated to be more than 216,800 tons Mo (Huang et al., 1989).

Since the discovery of the Lanjiagou Mo deposit, many scientific studies have been conducted, especially on the geology and geochemistry of the Mo ores (Ai and Feng, 1985; Ye and Wang, 1985; Luo et al., 1991; Yu, 1992; Dai et al., 2007; Tian, 1999), including studies on radiogenic isotopic dating and stable isotopes (Huang et al., 1996; Ai and Feng, 1985), and the ore-forming environments (Huang et al., 1996; Pei et al., 1998; Mao et al., 2003; Dai et al., 2006; Ge et al., 2007). However, much of the documentation of the Lanjiagou deposit has been reported in the Chinese literature, and the international geological community knows little about this deposit.

In the present study, we carried out Re–Os dating investigations on molybdenum ores from the Lanjiagou deposits in order to further constrain the timing of mineralization. In addition, we also discuss the geodynamic environments and processes that controlled the ore formation. An understanding of these mineralizing processes and geodynamic environments has important implications for the Mo exploration programs in the eastern part of the NCC.

2. Geological setting

The NCC is triangular in shape with an area of approximately 1,500,000 km^2, and is bounded by faults and younger orogenic belts (Fig. 1; Zhao et al., 2001). The Early Paleozoic Qilianshan Orogen and the Late Paleozoic–Late Mesozoic Tianshan–Inner Mongolia–Daxinganling Orogen bound the NCC to the west and the north, respectively (Fig. 1; Ren, 1980; Zorin et al., 2001; Zhao et al., 2001), and the Qinling–Dabie–Sulu ultrahigh-pressure metamorphic belt separates the NCC from the Yangtze Craton to the south and east (Fig. 1). Recently, many new results from investigations of magmatism, metamorphism, structure and tectonics, geochronology, and major, trace, and isotope geochemistry on rocks related to the NCC have been

* Corresponding author.
E-mail address: cm-han@mail.igcas.ac.cn (C. Han).

1342-937X/$ – see front matter © 2009 Published by Elsevier B.V. on behalf of International Association for Gondwana Research.
doi:10.1016/j.gr.2009.01.001

Table 1
Summary of geological and mineralogical features of molybdenum and copper deposits in the Yanshan–Liaoning metallogenic belt.

Deposits	Genetic types	Economic metals	Host rocks	Intrusive rocks	Wall–rock alteration	Reserve, grade	Orebody size	Sulfide assemblages	References
Yangjiazhangzi	Skarn	Mo	Middle-Upper Cambrian-Ordovi: limestone, shale and skarn	Porphyritic granite, granite–porphyry	Silicification, pyritization, chloritization, carbonization	26.2×10^4 Mo Mo: 0.14%	Length: 300–800 m Thickness: 3–10 m Depth: 200–250 m	Molybdenite, pyrite, Chalcopyrite, galena, zinc blende	Huang et al., 1989
Lanjiagou	Porphyry	Mo	Sinian: Dolomitic limestone, chert–dolomitic limestone; Cretaceous:pyroclastic rock	Porphyritic granite	k-feldspar alteration, greisenization, silicification, pyritization, chloritization, carbonization	21.68×10^4 Mo Mo: 0.13%	Length: 360–1280 m Thickness: 13–31 m Depth: 200–550 m	Molybdenite, pyrite, chalcopyrite, galena, magnetite, argentite	Huang et al., 1989
Xiaojiayingzi	Porphyry–skarn	Mo–Fe	Sinian: Dolomitic limestone, chert–dolomitic limestone	Porphyritic diorite	Skarnization, k-feldspar alteration, pyritization, carbonization, sericitization, chloritization	10.5×10^4 Mo Mo: 0.28%; 296.3×10^4 Fe Fe: 33.4%	Length: 150–800 m Thickness: 7–21 m Depth: 150–600 m	Molybdenite, pyrite, magnetite, chalcopyrite, galena, zinc blende	Dai et al., 2006
Dazhuangke	Porphyry	Mo	Sinian: Carbonate rock	Kjelsasite	K-feldspar alteration, silicification, pyritization, sericitization, chloritization	1.04×10^4 Mo Mo: 0.08%;	Length: 350–1000 m Thickness: 20–95 m Depth: 350–500 m	Molybdenite, pyrite, zinc blende, ilmenite, chalcopyrite,	Dai et al., 2006
Dawan	Porphyry–skarn	Mo–Cu–Zn–Ag	Sinian: Dolomitic limestone	Rhyolite porphyry	K-feldspar alteration, silicification, skarnization, Serpentinization, carbonization	25.9×10^4 Mo Mo: 0.12%	Length: $n\times1000$ m Thickness: $n\times10$ m Depth: $n\times100$ m	Molybdenite, pyrite, pyrrhotite, zinc blende, galena, chalcopyrite	Dai et al., 2006
Xiaosigou	Porphyry–skarn	Mo–Cu	Sinian: Dolomitic limestone, chert–dolomitic limestone	Granodiorite–porphyry	K-feldspar alteration, pyritization, skarnization, Serpentinization, sericitization	5.98×10^4 Mo Mo: 0.09%; 1.85×10^4 Cu Cu: 0.74%	Length: 2000 m Thickness: 30–100 m Depth: 300–500 m	Chalcopyrite, Chalcocite, pyrite, molybdenite, bornite, tetrahedrite	Dai et al., 2006
Shouwangfen	Skarn	Cu–Mo–Fe	Sinian: Dolomite, chert–dolomiteic	Porphyritic–granodiorite	Skarnization, chloritization, Sericitization, silicification, serpentinization	0.22×10^4 Mo Mo: 0.31%; 1.62×10^4 Cu Cu: 0.72%	Length: 200–500 m Depth: 150–300 m	Chalcopyrite, bornite, molybdenite, magnetite, zinc blende, galena	Dai et al., 2006

obtained (Hou et al., 2008a,b; Kusky et al., 2007; Peng et al., 2007; Santosh et al., 2007a,b; Zhai et al., 2007; Su et al., 2008).

The basement of the NCC has been divided into the Eastern and Western Blocks separated by the Paleoproterozoic Trans-North China Orogen (Fig. 1; Zhao et al., 2001). The Eastern Block consists of the Archean basement and the Paleoproterozoic Jiao-Liao-Ji Belt (Fig. 1; Zhao et al., 2005), and the Western Block can be subdivided into the Ordos and Yinshan Blocks separated by the Paleoproterozoic Khondalite Belt (Fig. 1; Zhao et al., 2005). There is a broad consensus that both the Khondalite Belt in the Western Block and the Trans-North China Orogen in the central part of the craton represent two Paleoproterozoic continent–continent collisional belts (Zhao et al., 2001, Wilde et al., 2002; Kröner et al., 2005, 2006). The Paleoproterozoic Khondalite Belt is considered to have formed by the amalgamation of the Yinshan Block in the north and the Ordos Block in the south to form the Western Block at 1.95–1.92 Ga (Zhao et al., 2005; Wan et al., 2006; Santosh et al., 2007a,b), and subsequently the Western Block collided with the Eastern Block along the Trans-North China Orogen to form the coherent basement of the NCC at ~1.85 Ga (Zhao et al., 2000, 2001, 2005; Guo et al., 2005; Liu et al., 2006).

The Early Archean basement rocks are only reported from the Eastern Block, represented by 3.5–3.85 Ga detrital zircons and fuchsite-bearing quartzites and ~3.5 Ga amphibolites in the Caozhuang area of the Eastern Hebei, and the 3.3–3.8 Ga granitoids and metasedimentary rocks in Anshan area (Liu et al., 1992; Song et al., 1996). Middle Archean basement rocks also mainly crop out in the Eastern Block, ranging in age from 3.5 to 3.0 Ga (Huang et al., 1986; Jahn et al., 1987; Kröner et al., 1988; Wu et al., 1991; Shen and Qian, 1995), and occurring as enclaves, boudins and sheets within the 2.6–2.5 Ga trondhjemite–tonalite–granodiorite (TTG) and 2.5 Ga syntectonic granites which make up much of the NCC (Wu et al., 1991; Kröner et al., 1988; Zhao et al., 2001). The late Archean basement rocks are widespread in both the Eastern Block and the Yinshan Block and consist predominantly of 2.8–2.5 Ga tonalitic–trondhjemitic–granodioritic (TTG) gneisses, ultramafic to mafic igneous intrusions, dykes and minor amounts of supracrustal rocks. Of these rocks, TTG gneisses make up 70% of the total exposure of the Neoarchean basement (Wu et al., 1991; Zhao et al., 1998), and the supracrustal rocks comprise sedimentary and bimodal volcanic rocks (Zhao et al., 1998). All these rocks were deformed and metamorphosed to between greenschist and granulite facies at 2.48–2.50 Ga (Jahn et al., 1987; Wu et al., 1991; Zhao et al., 1998; Ge et al., 2003).

Since the final cratonization at ~1.85 Ga (Zhao et al., 2001; Kusky et al., 2007), the NCC was subsequently covered by thick sequences of Meso-Neoproterozoic and Paleozoic sediments(Lu et al., 2008), with intrusions of diamondiferous kimberlites in Shandong and Liaoning Provinces during middle Ordovician time. The eastern part of the NCC became tectonically active again during Late Mesozoic time, with large-scale magmatism, basin development, ductile deformation and movement on large-scale faults which took place from the Late Jurassic to Early Cretaceous (Yang et al., 2003). In the Cenozoic, alkali basalts (many containing xenoliths) and minor tholeiitic basalts

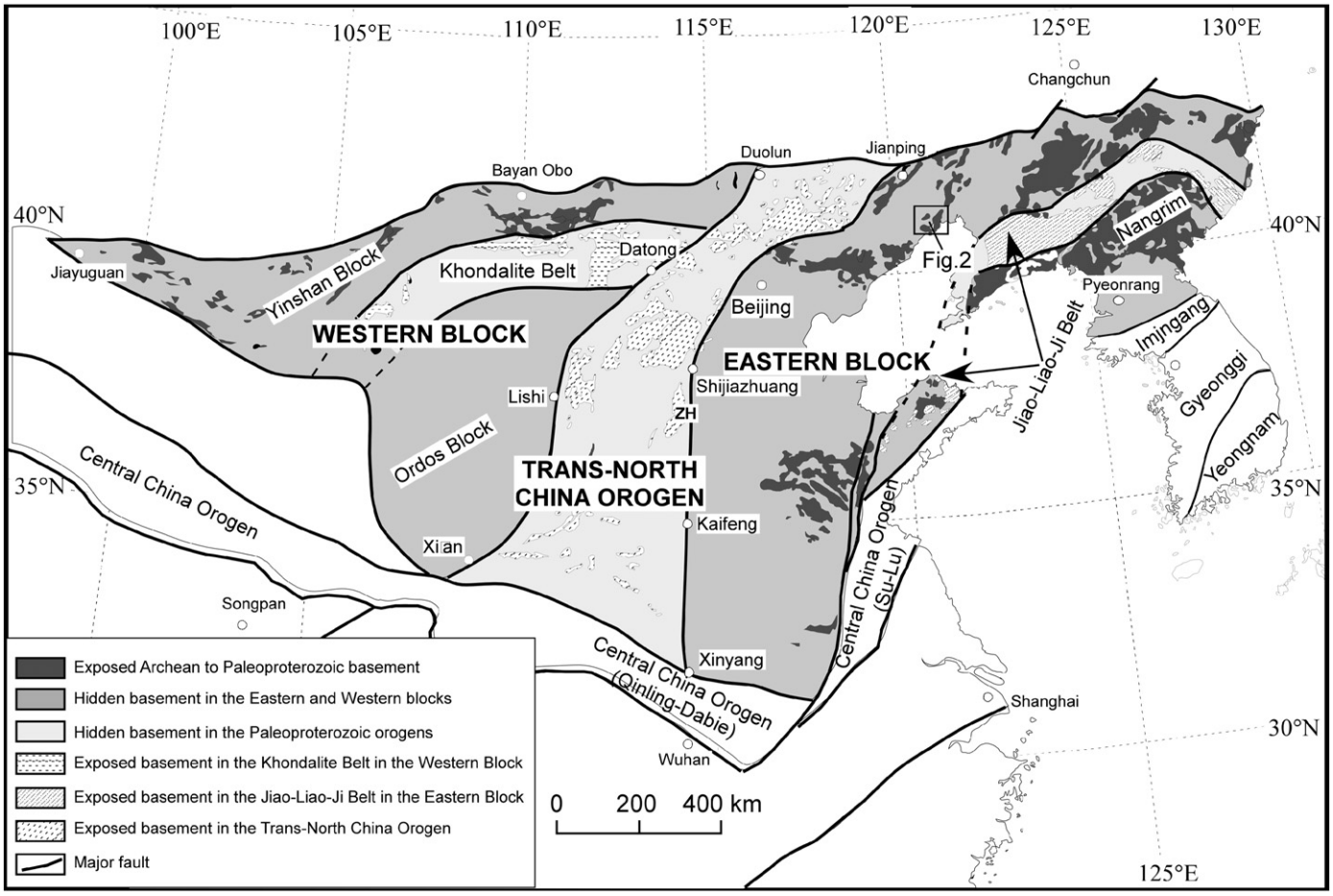

Fig. 1. Tectonic subdivision of the North China Craton (after Zhao et al., 2005). Fig. 2 is outlined.

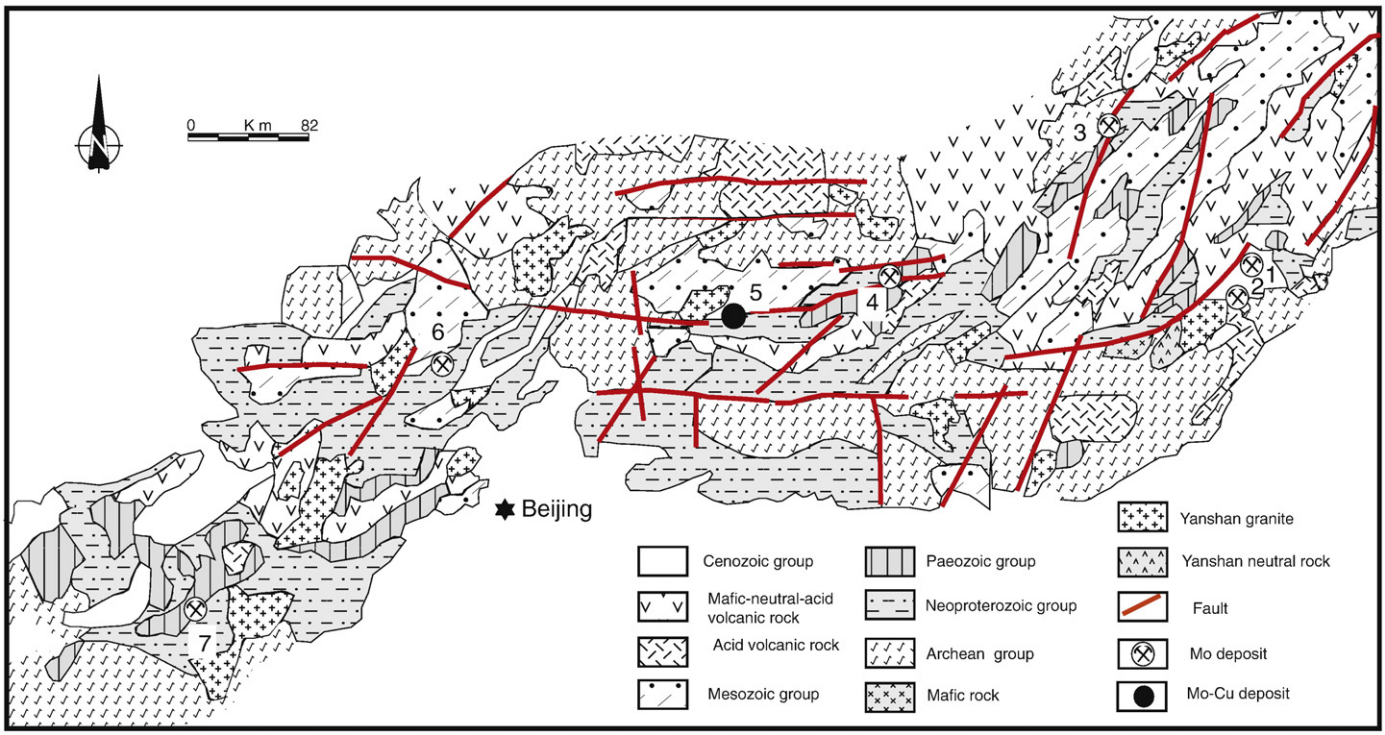

Fig. 2. Schematic geological map of the Yanshan–Liaoning molybdenum metallogenic belt on the northern margin of the North China platform (modified from Huang et al., 1996).

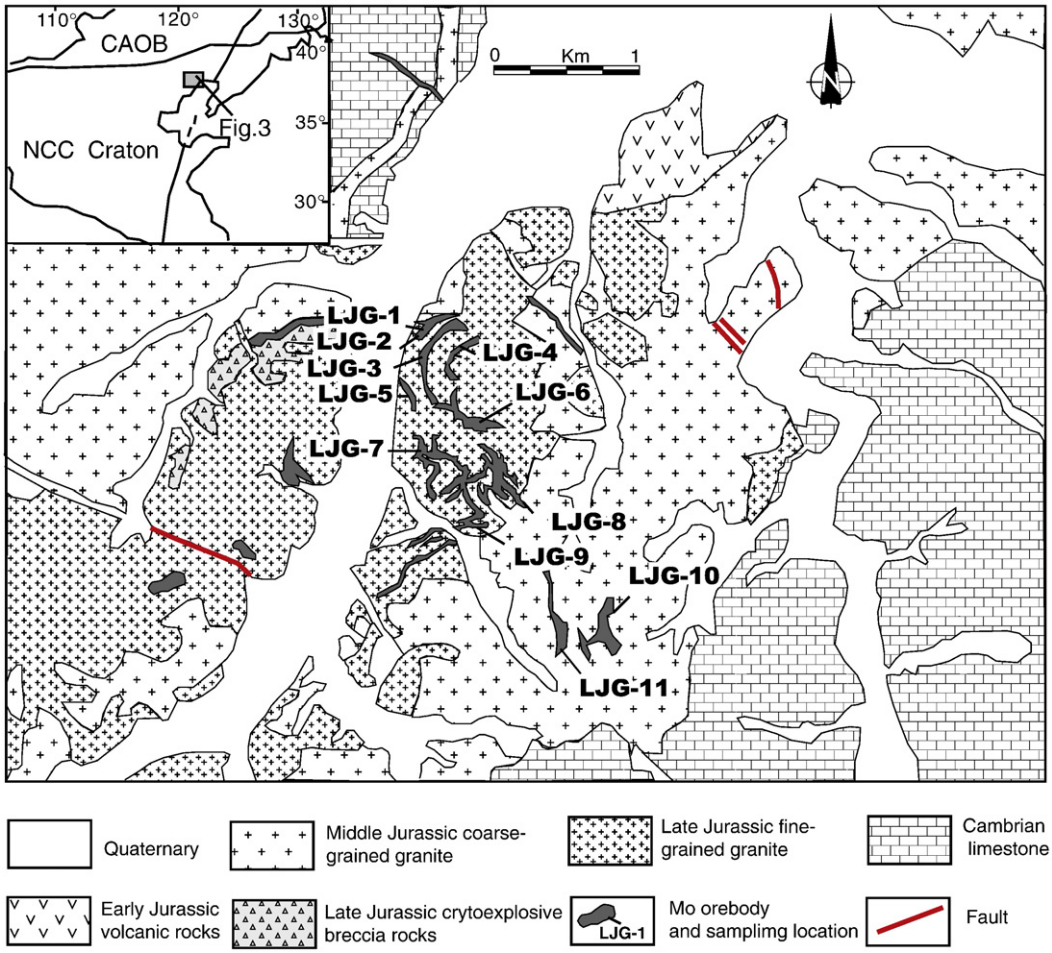

Fig. 3. Geological map of the Lanjiagou Mo deposit (modified from Dai et al., 2007).

erupted at several locations in the NCC (Basu et al., 1991; Tatsumoto et al., 1992).

The occurrence of diamondiferous kimberlites in Shandong and Liaoning Provinces suggests the presence of a thick and cold lithospheric root (ca. 200 km) of the NCC at least as late as Middle Ordovician time (Zhou et al., 1991, 1994; Menzies et al., 1993; Griffin et al., 1998). However, constraints from xenoliths in the Cenozoic basalts indicate that the NCC is now underlain by a hot lithosphere varying between 120 and 50 km thick (Ma et al., 1984), which is consistent with the available seismic and surface heat flow data. Therefore, it is evident that there was strong lithospheric thinning during Phanerozoic time, mostly in the Mesozoic and Cenozoic (Menzies et al., 1993; Menzies and Xu, 1998; Griffin et al., 1998), which is confirmed by the recent Os isotope studies of Gao et al. (2002) and Wu et al. (2003).

3. Lanjiagou Mo (copper) deposit

The Lanjiagou intrusion is composed of coarse-grained granite and fine-grained granite, the largest of which occupies a surface outcrop of ~20 km^2 (Fig. 3). Viewed from the surface outcrop, the intrusion is mostly irregular in shape, but viewed from the vertical section, the intrusion occurs as veins of larger bodies. The coarse-grained granite generally contains 40–45% orthoclase, 15–20% plagioclase, 30–33% quartz, and 3–5% biotite, with minor amounts of calcite, muscovite and sericite. The fine-grained granite generally contains 40–45% orthoclase, 15–20% plagioclase, 28–35% quartz, and 1–3% biotite, with minor amounts of calcite, muscovite and epidote. Orthoclase crystals range from 0.36 to 3.5 mm in size. Geochronology of coarse-grained granite ranges between 178 and 186 Ma K–Ar method, and the fine-grained granite yields a Rb–Sr whole-rock isochron age of 154 ± 14 Ma.

The Lanjiagou deposit can be further subdivided into the upper Lanjiagou, Middle Lanjiagou, Lower Lanjiagou, Xiaomagou, Yuanbaoshan and Xishan districts. Totally 101 mineralized bodies have been identified, and they are distributed in the middle segment of the fine-grained granite and the contact zone between the coarse-grained and fine-grained granites. Individual ore bodies vary from 76 m to 1288 m in length and 3.1 m to 31.8 m in thickness. In the dipping direction, the explored ore bodies extend over 400 m below the surface. The main ore bodies trend in NW and NS with a dip angle about 45°. The size of molybdenite ranges from 0.01 mm to 0.15 mm. The ores are characterized by euhedral and subhedra textures, veinlet-disseminated and brecciated structures. Principal metallic minerals are molybdenite and pyrite as well as minor quantities of zinc blende, chalcopyrite, galena, magnetite and electrum. The gangue minerals include mainly orthoclase, plagioclase and quartz, with lesser amounts of calcite, muscovite and chlorite. Wall rocks alteration is marked by silicification, sericitization, carbonatization, chloritization, potassic alteration and greisenization (Luo et al., 1991).

According to mineral assemblages and crosscutting relationships of the ore veins, five mineralization stages can be identified (Fig. 4). The first mineralization stage (I) is characterized by gas–liquid metasomatism, accompanied by potassium feldspar, quartz and muscovite. The second stage (II) is characterized mainly by phyllic alteration, forming the quartz + sericite + magnetite + pyrite assemblage that occurs as veins. The third stage (III, main mineralization stage) is represented by the formation of veins containing quartz + molybdenite + pyrite + sphalerite. The fourth stage (IV) is marked by the formation of the

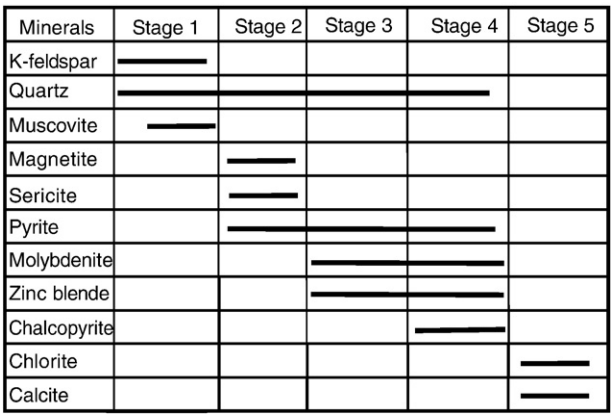

Fig. 4. Paragenesis sequence of minerals of the Lanjiagou Mo deposit (modified from Luo et al., 1991).

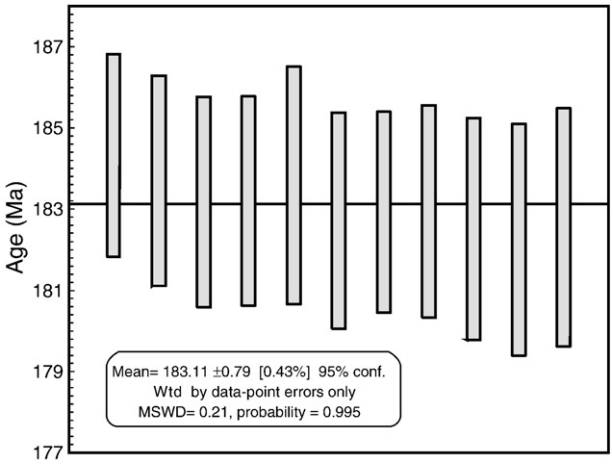

Fig. 5. Re–Os ages for molybdenite from the Lanjiagou porphyry molybdenum deposit in the eastern NCC.

quartz + molybdenite + pyrite + sphalerite assemblage that occurs as veins and disseminated by barren calcite–quartz veins. The fifth stage (V) is characterized by the presence of carbonate(calcite) + chlorite + minor sulfides (Luo et al., 1991).

4. Sampling and analytical methods

We selected 11 samples from the Lanjiagou deposit for Re–Os dating (Fig. 3), all of which were collected from fresh open-pit mining faces. Sampling locations are marked in Fig. 4. Gravitational and magnetical separation was applied and then handpicked under a binocular microscope (purity>99%). The molybdenite in the samples is fine grained (<0.1 mm), thus avoiding the decoupling of Re and Os within large molybdenite grains (Stein et al., 2003; Selby and Creaser, 2004).

Re–Os isotopic analyses were performed at the National Research Center of Geoanalysis, Chinese Academy of Geosciences. The details of the chemical procedure have been described by Du et al. (1995, 2001), Shirey and Walker (1995), Stein et al. (1998) and Markey et al. (1998) and are briefly summarized below.

Enriched ^{190}Os and enriched ^{185}Re were obtained from the Oak Ridge National Laboratory, USA. A Carius tube (a thick-walled borosilicate glass ampoule) digestion was used. The weighed sample was loaded in the Carius tube through a thin neck long funnel. The mixed ^{190}Os and ^{185}Re spike solutions and 2 ml of 12 M HCl. and 6 ml of 15 M HNO_3 were loaded while the bottom part of the tube was frozen at −80 to −50 °C in an ethanol–liquid nitrogen slush; the top was sealed using an oxygen–propane torch. The tube was then placed in a stainless-steel jacket and heated for 24 h at 230 °C. Upon cooling, the bottom part of the tube was kept frozen, the neck of the tube was broken, and the contents of the tube were poured into a distillation flask and the residue was washed out with 40 ml of water.

Osmium was distilled at 105–110 °C for 50 min and trapped in 10 ml of water. The residual Re-bearing solution was saved in a 150 ml Teflon beaker for Re separation. The water trap solution was used for ICP-MS (TJA X-series) determination of the Os isotope ratio.

The Re-bearing solution was evaporated to dryness, and 1 ml of water was added twice with heating to near-dryness in between 10 ml of 20% NaOH was added to the residue followed by Re extraction with 10 ml of acetone in a 120 ml Teflon separation funnel. The water phase was then discarded and the acetone phase washed with 2 ml of 20% NaOH. The acetone phase was transferred to a 120 ml Teflon beaker that contained 2 ml of water. After evaporation to dryness, the Re was picked up in 1 ml of water that was used for the ICP-MS determination of the Re isotope ratio. Cation-exchange resin was used to remove Na if the salinity of the Re-bearing solution was more than 1 mg/ml (Du et al., 2004).

The ICP-MS measurement condition is below: the instrument used for this analysis was a TJA PQ ExCELL ICP mass spectrometer. The instrument was optimized to: $>5\times10^4$ cps for 1 ng ml^{-1} ^{115}In and $>5\times10^4$ cps for 1 ng ml^{-1} ^{238}U. The operating conditions are that the data acquisition: peak-jumping mode, 3 points/u; dwell time:15 ms/point; number of scan: 200 for 5 ppb of Re solution, the reproducibility by ICP-MS to be 0.3% (RSD, 2S, $n=5$); by using water as an absorbent for OsO_4, the sensitivity of Os by ICP-MS increases a lot. For 0.2 ppb of Os solution, the reproducibility is 0.3% (RSD, 2S, $n=5$).

If a minor ^{190}Os signal was observed when measuring Re, the ^{187}Re signal was appropriately corrected for ^{187}Os using the ^{187}Os/^{190}Os ratio of the spiked Os solution. Conversely, if a minor ^{185}Re signal was

Table 2
Re–Os isotopic data for molybdenite from the Lanjiagou Mo deposit, eastern China.

No. samples	Weight (g)	Re (μg/g)		^{187}Re (μg/g)		^{187}Os (ng/g)		Model age (Ma)	
		Measured	2σ	Measured	2σ	Measured	2σ	Measured	2σ
LJG-1	0.10654	36.07	0.33	22.67	0.21	69.29	0.53	183.2	2.6
LJG-2	0.11245	45.83	0.41	28.81	0.26	88.06	0.67	183.2	2.6
LJG-3	0.10013	33.29	0.37	20.93	0.23	64.10	0.53	183.6	2.9
LJG-4	0.10083	40.53	0.36	25.47	0.23	77.66	0.67	182.7	2.7
LJG-5	0.10143	33.96	0.26	21.35	0.17	65.16	0.52	182.9	2.5
LJG-6	0.10028	37.49	0.34	23.56	0.21	71.93	0.56	182.9	2.6
LJG-7	0.10041	35.59	0.36	22.37	0.23	68.13	0.54	182.5	2.7
LJG-8	0.10012	36.25	0.39	22.78	0.24	69.29	0.58	182.3	2.9
LJG-9	0.10048	47.85	0.50	30.08	0.31	91.62	0.88	182.6	2.9
LJG-10	0.02396	35.83	0.29	22.52	0.18	69.28	0.52	184.3	2.5
LJG-11	0.02368	35.05	0.31	22.03	0.20	67.53	0.52	183.7	2.6

Decay constant: λ (^{187}Re) = 1.666×10^{-11}/year (Smoliar et al., 1996). The uncertainty in each individual age determination was about 1.5% including the uncertainty of the decay constant of ^{187}Re, uncertainty in isotope ratio measurement, and spike calibration.

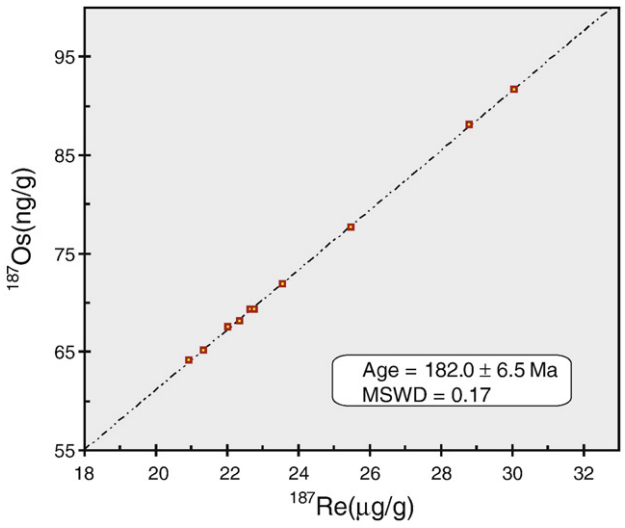

Fig. 6. Re–Os isochron plot for molybdenite samples from the Lanjiagou Mo deposit, eastern NCC.

observed while analyzing the Os-bearing, ^{187}Os was appropriately corrected for ^{187}Re using the measured ^{185}Re/^{187}Re of the spiked sample. The corrections were generally minor and constituted no more than 0.1% of the isotope signal. The maximum correction percentage that we used is less than 1%.

The mass fractionation can be corrected using an interlaboratory isotope reference standard. Using the λ^{238}U value of Jaffey et al. (1971) and λ^{235} value of Schoene et al. (2006), a value for λ^{187}Re of $1.6689 \pm 0.0031 \times 10^{-11}$ a^{-1} is determined. These values are nominally higher (ca. 0.1% and ca. 0.2%) than the value determined by Smoliar et al. (1996), but within calculated uncertainty. So, we still use the λ^{187}Re $1.666 \pm 0.005 \times 10^{-11}$ a^{-1} determined by Smoliar et al. (1996).

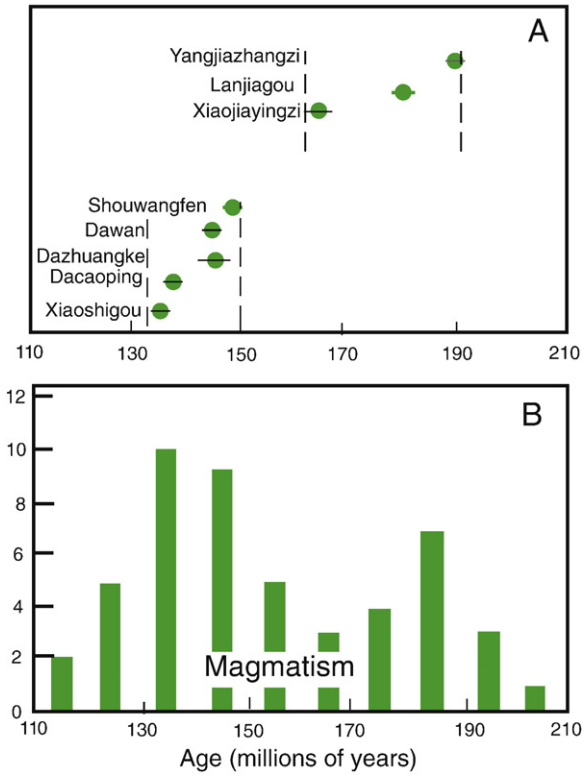

Fig. 7. (A) Time span of mineralization (diamonds) ages for the Yanshan–Liaoning base metal porphyry–skarn deposits. (B) Histogram of Yanshan–Liaoning magmatism (number of age determinations) for eastern NCC, with intervals of base metal porphyry–skarn deposits indicated by crosshatched bands. Data are from Huang et al. (1996) and this study.

Average blanks for the total Carius tube procedure as described above were ca. 10 pg Re and ca. 0.1 pg Os. ^{187}Os was not detected. Three reference materials were used to inspect the analytical results.

The uncertainty in each individual age determination was about 1.4% including the uncertainty of the decay constant of ^{187}Re, uncertainty in isotope ratio measurement, and spike calibrations. The decay constant used for ^{187}Re of 1.666×10^{-11} a^{-1} has an absolute uncertainty of ±0.017 (1.0%) (Smoliar et al., 1996).

5. Results

Results of molybdenite Re–Os dating are listed in Table 2. The concentrations of Re and ^{187}Os range from 33.293 to 47.852 ppm and 64.103 to 91.617 ppb, respectively. Eleven samples give a Re–Os model age of 182.3–184.3 Ma and a weighted mean age of (183.11 ± 0.79) Ma (Fig. 5). The data, processed using the ISOPLOT/Ex program (Ludwig, 2004), yielded an isochron age of (181.6 ± 6.5) Ma, with MSWD = 0.31 and an initial ^{187}Os of 0.6 ± 2.5 ppb (Fig. 6). The nearly identical model age and isochron age suggest that the analytical results are reliable.

6. Intradeposit relations and regional timing of mineralization

Mo–Cu ore deposits in the eastern part of the NCC are mainly distributed in the northern Hebei–West Liaoning region. These deposits are restricted to two narrow intervals: ~190 Ma to 165 Ma and ~150 Ma to 130 Ma years ago (Fig. 7; Table 3). These intervals are irrespective of time of inception, or ore deposit size. In the Western Liao-Ning are, porphyry–skarn mineralization formed during from 165 Ma to 190 Ma.

Almost all porphyry-style deposits described in the literature are Phanerozoic and their formation is linked to magmatic activity at active plate margins (Titley and Beane, 1981). They can be divided into two main types: porphyry Cu–Mo and porphyry Cu–Au ± Mo deposits (Sillitoe, 1997). The first type is generally found in continental margin arcs, like the Andean belt, dominated by calc-alkaline intrusions. The second type is typical of continental margins or island arc terranes, such as those in the southwest Pacific region where calc-alkaline rocks or high-K, calc-alkaline rocks prevail (Sillitoe, 1997).

The eastern NCC became an active continental margin before Jurassic (Zhou and Li, 2000; Li and Li, 2007). Its geodynamic evolution was closely associated with the evolution of an ancient Pacific plate. From the Late Jurassic to Cretaceous, it was proposed that this margin was related to the subduction of the Pacific plate (Zhou and Li, 2000;

Table 3
Available geochronological data for ore deposits in East China.

Name of deposit	Dated minerals/ rocks	Dating method	Age (Ma)	Data sources
Xiaojiayingzi	Molybdenite	Re–Os isochron	165.5 ± 4.6	Dai et al. (2007)
"	Molybdenite	Re–Os isochron	177 ± 5	Huang et al. (1996)
Lanjiagou	Molybdenite	Re–Os isochron	181.6 ± 6.5	Huang et al. (1996)
"	Muscovite	K–Ar	178–186.3	Tian (1999)
Yangjiazhangzi	Molybdenite	Re–Os model	191 ± 6	Huang et al. (1996)
"	Molybdenite	Re–Os model	187 ± 2	Huang et al. (1996)
"	Muscovite	K–Ar	188.8	Tian (1999)
"	Adamellite	SHRIMP	188 ± 2	Wu et al. (2006)
Xiaoshigou	Molybdenite	Re–Os model	134 ± 3	Huang et al. (1996)
"	Gabbro-diabase	K–Ar	188.8	Tian (1999)
Shouwangfeng	Molybdenite	Re–Os model	148 ± 4	Huang et al. (1996)
Dawan	Molybdenite	Re–Os model	144.4 ± 7.4	Huang et al. (1996)
Dazhuangke	Molybdenite	Re–Os model	147.1 ± 6.68	Huang et al. (1996)
"	Molybdenite	Re–Os model	144.7 ± 10.7	Huang et al. (1996)
"	Molybdenite	Re–Os model	146.4 ± 5.9	Huang et al. (1996)
Sandaozhuang	Molybdenite	Re–Os model	144.5 ± 2.2	Mao et al. (2006)
"	Molybdenite	Re–Os model	145.0 ± 2.2	Mao et al. (2006)
"	Molybdenite	Re–Os model	145.4 ± 2.0	Mao et al. (2006)

Zhu et al., 2005; Zhou et al., 2006) in the south, concurrent with oblique subduction of the Izanagi plate in the north (Maruyama et al., 1997). With regard to regional timing mineralization, some clues to understanding the processes involved are given by observation that base metal porphyries are spatially and temporally associated with the subduction of oceanic lithosphere (Sawkins, 1990).Upon subduction, the oceanic lithosphere undergoes dehydration and partial melting. The partial melts and volatiles rise and interact with overlying continental lithosphere and promote partial melting in the lower crust. Some of the magma produced by the interaction ascends higher into the upper crust, forming the volcanic rock if it breaches the surface or an intrusion if it cools beneath the surface. In Jurassic times, magmatism associated with Izanagi plate is ubiquitous in the east NCC.

Portions of these mixed magmas reached the upper crust as flows or intrusions. The lower crust underwent further melting as new volatiles or partial melting rose from the mantle in response to the subducting Izanagi plate. As remelting of the residues continued in the lower crust, some components accumulated that are crucial for the formation of base porphyry–skarn deposits. Eventually a magma evolved that contained these components (metals as well as sulfur, water, or both) in sufficient amounts that, upon their emplacement into the upper crust, a base metal porphyry deposit formed. This critical abundance level was achieved in the West Liaoning crust ~190 Ma to 165 Ma years ago and in the North Hebei Crust ~150 Ma to 130 Ma years ago. Magmatism of similar age and duration is common the two Precambrian basement domains, but base metal porphyry mineralization is restricted to two different intervals specific to those domains. The processes leading to the regional timing of mineralization were probably not instantaneous but evolutionary, creating windows of time which magmas that reached the upper crust would contain the components necessary for the formation of base metal porphyry–skarn deposit.

7. Conclusions

(1) Eleven molybdenites yielded an isochron age of 181.6 ± 6.5 Ma (2σ) with an initial ^{187}Os of 0.6 ± 2.5 (MSWD = 0.31), model ages for individual analyses range from 182–184 Ma;
(2) Combined with the regional geological history, the evolution of the porphyry Mo deposit in the Lanjiagou area and associated Mo mineralization during Mesozoic time were closely related to the subduction of the Pacific plate.

Acknowledgements

We are indebted to Bin Cui, Jinwen Mao, Kezhang Qin, Zhaochong Zhang, Lian-Chang Zhang, Zongyao Rui, Zhiliang Wang, and Jianming Yang for discussions. Many of the ideas in this paper were initiated and rectified during these discussions. This study was financially supported by funds from the Chinese State 973 Project (2007CB411307), the NSFC Project (40725009, 40421303, and 40572043), the State Key Laboratory of Lithospheric Evolution, the Chinese State 973 Project (2001CB409801) and Hong Kong RGC (7066/07P). This paper is a contribution to the ILP (ERAS) and IGCP 480.

References

Ai, Y.F., Feng, R.Z., 1985. Mo-bearing granitic material Sources and genetic type of Yangjiazhangzi–Lanjiagou. Henan Geology (Supp.) 198–204 (in Chinese with English abstract).
Basu, A.R., Wang, J.W., Huang, W.K., Xie, G.H., Tatsumoto, M., 1991. Major element, REE, and Pb, Nd and Sr isotopic geochemistry of Cenozoic volcanic rocks of eastern China: implications for their origin from suboceanic-type mantle reservoirs. Earth and Planetary Science Letters 105, 149–169.
Dai, J.Z., Mao, J.W., Yang, F.Q., Ye, H.S., Zhao, C.S., Xie, G.Q., Zhang, C.Q., 2006. Geological characteristics and geodynamic background of molybdenum (copper)deposits along Yanshan–Liaoning metallogenic belt on northern margin of North China block. Mineral Deposits 25, 598–612 (in Chinese with English abstract).
Dai, J.Z., Mao, J.W., Xie, G.Q., Yang, F.Q., Zhao, C.S., 2007. Ore-forming fluid characteristics and genesis of Lanjiagou molybdenum deposit in western Liaoning Province. Mineral Deposits 26, 443–454 (in Chinese with English abstract).
Du, A.D., He, H.L., Yin, N.W., 1995. A study of the rhenium–osmium geochronometry of molybdenites. Acta Geologica Sinica 8, 171–181.
Du, A.D., Wang, S.X., Sun, D., Zhao, D., Liu, D., 2001. Precise Re–Os dating of molybdenite using Carius tube, NTIMS and ICPMS. In: Piestrzynski (Ed.), Mineral Deposits at the 21st Century, pp. 405–407.
Du, A.D., Wu, S.Q., Sun, D.Z., Wang, S.X., Qu, W.J., Markey, R., Stein, H., Morgan, J.W., Malinovskiy, D., 2004. Preparation and certification of Re–Os dating reference materials: molybdenite HLP and JDC. Geostand. Geoanalysis Research 28, 41–52.
Gao, S., Rudnick, R.L., Carlson, R.W., McDonough, W.F., Liu, Y.S., 2002. Re-Os evidence for replacement of ancient mantle lithosphere beneath the north China Craton. Earth and Planetary Science Letters 198, 307–322.
Ge, W.C., Zhao, G.C., Sun, D.Y., Wu, F.Y., Lin, Q., 2003. Metamorphic P–T path of the Southern Jilin complex: implications for tectonic evolution of the Eastern block of the North China craton. International Geology Review 45, 1029–1043.
Ge, W.C., Wu, F.Y., Zhou, C.Y., Zhang, J.H., 2007. Porphyry Cu–Mo deposits in the eastern Xing'an-Mongolian Orogenic Belt: mineralization ages and their geodynamic implications. Chinese Science Bulletin 52, 3416–3427.
Griffin, W.L., Zhang, A., O'Reilly, S.Y., Ryan, C.G., 1998. In: Flower, M.F.J., Chung, S.-L., Lo, C.-H., Lee, T.-Y. (Eds.), Phanerozoic Evolution of the Lithosphere Beneath the Sino - Korean Craton. . Mantle Dynamics and Plate Interactions in East Asia-Geodynamics Series, vol. 27. American Geophysical Union, Washington DC, pp. 107–126.
Guo, J.H., Sun, M., Zhai, M.G., 2005. Sm–Nd and SHRIMP U–Pb zircon geochronology of high-pressure granulites in the Sanggan area, North China Craton: timing of Paleoproterozoic continental collision. Journal of Asian Earth Science 24, 629–642.
Hou, G.T., Li, J., Yang, M., Yao, W., Wang, C., Wang, Y., 2008a. Geochemical constraints on the tectonic environment of the Late Paleoproterozoic mafic dyke swarms in the North China Craton. Gondwana Research 13, 103–116.
Hou, G.T., Santosh, M., Qian, X.L., Lister, G.S., Li, J.H., 2008b. Tectonic constraints on 1.3~1.2 Ga final breakup of Columbia supercontinent from a giant radiating dyke swarm. Gondwana Research 14, 561–566.
Huang, X., Bai, Z., DePaolo, D.J., 1986. Sm–Nd isotope study of Early Archean rocks, Qianan, Hebei Province, China. Geochimica et Cosmochimica Acta 50, 625–631.
Huang, D.H., Dong, Q.Y., Gan, Z.X., 1989. China molybdenum deposits. In: Song, S.H. (Ed.), China Deposits (Vol.1). Beijing: Geo1ogy Publishing House, pp. 493–536 (in Chinese with English abstract).
Huang, D.H., Wu, C.Y., Du, A.D., He, H.L., 1994. Re–Os ages molybdenum deposits in east Qinling and their significance. Mineral Deposits 13, 221–230 (in Chinese with English abstract).
Huang, D.H., Du, A.D., Wu, C.Y., Liu, L.S., Sun, Y.L., Zou, X.Q., 1996. Metallochronology of molybdenum (copper) deposits in the north China platform: Re–Os age of molybdenite and its geological significance. Mineral Deposits 15, 289–297 (in Chinese with English abstract).
Jaffey, A.H., Flynn, K.F., Glendenin, L.E., Bentley, W.C., Essling, A.M., 1971. Precision measurement of half-lives and specific activities of ^{235}U and ^{238}U. Physical Reviews 4, 1889–1906.
Jahn, B.M., Auvray, B., Cornichet, J., Bai, Y.L., Shen, Q.H., Liu, D.Y., 1987. 3.5 Ga old amphibolites from eastern Hebei Province, China: field occurrence, petrography, Sm–Nd isochron age and REE geochemistry. Precambrian Research 34, 311–346.
Kröner, A., Compston, W., Zhang, G.W., Guo, A.L., Todt, W., 1988. Ages and tectonic setting of Late Archean greenstone–gneiss terrain in Henan Province, China, as revealed by single-grain zircon dating. Geology 16, 211–215.
Kröner, A., Wilde, S.A., Li, J.H., Wang, K.Y., 2005. Age and evolution of a late Archaean to early Palaeozoic upper to lower crustal section in the Wutaishan/Hengshan/Fuping terrain of northern China. In: Wilde, S.A., Zhao, G.C. (Eds.), Late Archean to Paleoproterozoic evolution of the North China Craton. Journal of Asian Earth Science, vol. 24, pp. 577–595.
Kröner, A., Wilde, S.A., Zhao, G.C., O'Brien, P.J., Sun, M., Liu, D.Y., Wan, Y.S., Liu, S.W., Guo, J.H., 2006. Zircon geochronology of mafic dykes in the Hengshan Complex of northern China: evidence for late Palaeoproterozoic rifting and subsequent high-pressure event in the North China Craton. Precambrian Research 146, 45–67.
Kusky, T., Li, J.H., Santosh, M., 2007. The Paleoproterozoic North Hebei Orogen: North China craton's collisional suture with the Columbia supercontinent. Gondwana Research 12, 4–28.
Li, Z.X., Li, X.H., 2007. Formation of the 1300-km-wide intracontinental orogen and postorogenic magmatic province in Mesozoic South China: a flat-slab subduction model. Geology 35, 179–182.
Liu, D.Y., Nutman, A.P., Compston, W., Wu, J.S., Shen, Q.H., 1992. Remnants of >3800 Ma crust in the Chinese part of the Sino- Korean craton. Geology 20, 339–342.
Liu, S.W., Zhao, G.C., Wilde, S.A., Shu, G.M., Sun, M., Li, Q.G., Tian, W., Zhang, J., 2006. Th–U–Pb monazite geochronology of the Luliang and Wutai Complexes: constraints on the tectonothermal evolution of the Trans-North China Orogen. Precambrian Research 148, 205–225.
Lu, S.N., Zhao, G.C., Wang, H.C., Hao, G.J., 2008. Precambrian metamorphic basement and sedimentary cover of the North China Craton: review. Precambrian Research 160, 77–93.
Ludwig, K.R., 2004. Isoplot/Ex, Version 3.0: a Geochronological Toolkit for Microsoft Excel. Berkeley Geochronology Center, Berkeley, CA.
Luo, M.J., Zhang, F.M., Dong, Q.Y., Xu, Y.R., Li, S.M., Li, K.H., 1991. China Molybdenum Deposits. Zhengzhou: Henan Science and Technology Press. 1-425 (in Chinese with English abstract).
Ma, X.Y., Liu, G., Su, J., 1984. The structure and dynamics of the continental lithosphere in north - northeast China. Annals of Geophysics 2, 611–620.

Mao, J.W., Zhang, Z.H., Yu, J.J., Wang, Y.T., Niu, B.G., 2003. The geodynamic setting of Mesozoic large-scale mineralization in North China: the revelation from accurate timing of metal deposits. Science in China (Ser. D) 33, 289–300 (in Chinese).

Mao, J.W., Wang, Y.T., Lehmann, B., Yu, J.J., Du, A.D., Mei, Y.X., Li, Y.F., Zang, W.S., Stein, H.J., Zhou, T.F., 2006. Molybdenite Re–Os and albite $_{40}Ar/_{39}Ar$ dating of Cu–Au–Mo and magnetite porphyry systems in the Yangtze River valleyand metallogenic implications. Ore Geology Reviews 29, 307–324.

Maruyama, S., Isozaki, Y., Kimura, G., Terabayashi, M., 1997. Paleogeographic maps of the Japanese Islands: plate tectonic synthesis from 750 Ma to the present. Island Arc 6, 121–142.

Markey, R., Stein, H., Morgan, J., 1998. Highly precise Re–Os dating for molybdenite using alkaline fusion and NTIMS. Talanta 45, 935–946.

Menzies, M.A., Fan, W.M., Zhang, M., 1993. In: Prichard, H.M., et al. (Ed.), Palaeozoic and Cenozoic Lithoprobes and the Loss of >120 km of Archean Lithosphere, Sino-Korean Craton, China. Magmatic Processes and Plate Tectonics. Special Publication-Geological Society, vol. 76, pp. 71–81.

Menzies, M.A., Xu, Y., 1998. In: Flower, M.F.J., Chung, S.-L., Lo, C.-H., Lee, T.-Y. (Eds.), Geodynamics of the North China Craton. . Mantle Dynamicas and Plate Interactions in East Asia. Geodynamics Series, vol. 27. American Geophysical Union, Washington DC, pp. 155–163.

Pei, R.F., Lv, X., Fan, J.Z., Fang, R.H., Qi, C.S., 1998. Metal Deposits Metallogeneitic Series and Prospecting of North Margin of the North China Massif and its North Side. Geo1ogy Publishing House, Beijing, pp. 1–237 (in Chinese with English abstract).

Ren, J.S., 1980. Tectonics and Evolution of China. Science Press, Beijing, pp. 64–75 (in Chinese).

Peng, P., Zhai, M.G., Guo, J.H., Kusky, T., Zhao, T.P., 2007. Nature of mantle source contributions and crystal differentiation in the petrogenesis of the 1.78 Ga mafic dykes in the central North China craton. Gondwana Research 12, 29–46.

Santosh, M., Tsunogae, T., Li, J.H., Liu, S.J., 2007a. Discovery of sapphirine-bearing Mg–Al granulites in the North China Craton: implications for Paleoproterozoic ultrahigh temperature metamorphism. Gondwana Research 11, 263–285.

Santosh, M., Wilde, S.A., Li, J.H., 2007b. Timing of Paleoproterozoic ultrahigh - temperature metamorphism in the North China Craton: evidence from SHRIMP U–Pb zircon geochronology. Precambrian Research 159, 178–196.

Sawkins, F.J., 1990. Metal Deposits in Relation to Plate Tectonics, 2nd ed. Spring-Verlag, Berlin.

Schoene, B., Crowley, J.L., Condon, D.J., Schmitz, M.D., Bowring, S.A., 2006. Reassessing the uranium decay constants for geochronology using ID-TIMS U–Pb data. Geochimica et Cosmochimica Acta 70, 426–445.

Selby, D., Creaser, A., 2004. Macroscale NTIMS and microscale LA-MC-ICP-MS Re–Os isotopic analysis of molybdenite: testing spatial restrictions for reliable Re–Os age determinations, and implications for the decoupling of Re and Os within molybdenite. Geochimica et Cosmochimica Acta 68, 3897–3908.

Shen, Q.H., Qian, X.L., 1995. Archean rock assemblages, episodes and tectonic evolution of China. Acta Geologica Sinica 2, 113–120 (in Chinese with English abstract).

Shirey, S.B., Walker, R.J., 1995. Carius tube digestion for low-bank rhenium–osmium analysis. Analysis Chemical 67, 2136–2141.

Sillitoe, R.H., 1997. Characteristics and controls of the largest porphyry Cu–Au and epithermal Au deposits in the circum-Pacific region. Australia Journal of Earth Science 44, 373–388.

Smoliar, M.I., Warker, R.J., Morgan, J.W., 1996. Re–Os ages of group IIA, IIIA, IVA and VIB iron meteorites. Science 271, 1099–1102.

Song, B., Nutman, A.P., Liu, D.Y., Wu, J., 1996. 3800 to 2500 Ma crustal evolution in the Anshan area of Liaoning Province, northeastern China. Precambrian Research 78, 79–94.

Stein, H.J., Sundblad, K., Markey, R.J., Motuza, G., 1998. Re–Os ages for Archean molybdenite and pyrite, Kuittila–Kivisuo, Finland, and Proterozoic molybdenite, Kabeliai, Lithuania: testing the chronometer in a metamorphic and metasomatic setting. Mineralium Deposita 33, 329–345.

Stein, H.J., Schersten, K., Hannah, J.L., Markey, R., 2003. Subgrain-scale decoupling of Re and $_{187}Os$ and assessment of laser ablation ICP-MS spot dating in molybdenite. Geochimica et Cosmochimica Acta 92, 827–835.

Su, W., Zhang, S., Huff, W.D., Li, H., Ettensohn, F.R., Chen, X., Yang, H., Han, Y., Song, B., Santosh, M., 2008. SHRIMP U–Pb ages of K-bentonite beds in the Xiamaling Formation: implications for revised subdivision of the Meso- to Neoproterozoic history of the North China Craton. Gondwana Research 14, 543–553.

Tatsumoto, M., Basu, A.R., Huang, W.K., Wang, J.W., Xie, G.H., 1992. Sr, Nd and Pb isotopes of ultramafic xenoliths in volcanic rocks of eastern China: enriched components EM1 and EM2 in subcontinental lithosphere. Earth and Planetary Science Letters 113, 107–128.

Tian, Y.C., 1999. Metallogenic structure, magmatic evolution and mineralizing process of molybdenum mineral area of Lanjiagou, west Liaoning. Mineral Resource and Geology 13, 135–140 (in Chinese with English abstract).

Titley, S.R., Beane, R.E., 1981. Porphyry copper deposits. Economic Geology, 75th Anniversary Volume, pp. 214–269.

Wan, Y.S., Song, B., Liu, D.Y., Wilde, S.A., Wu, J.S., Shi, Y.R., Yin, X.Y., Zhou, H.Y., 2006. SHRIMP U–Pb zircon geochronology of Palaeoproterozoic metasedimentary rocks in the North China Craton: evidence for a major Late Palaeoproterozoic tectonothermal event. Precambrian Research 149, 249–271.

Wilde, S.A., Zhao, G.C., Sun, M., 2002. Development of the North China Craton during the Late Archaean and its final amalgamation at 1.8 Ga; some speculations on its position within a global Palaeoproterozoic Supercontinent. Gondwana Research 5, 85–94.

Wu, J.S., Geng, Y.S., Shen, Q.H., Liu, D.Y., Li, Z.L., Zhao, D.M., 1991. The Early Precambrian Significant Geological Events in the North China Craton. Geological Publishing, Beijing, pp. 1–115 (in Chinese with English abstract).

Wu, F.Y., Walker, R.J., Ren, X.W., Sun, D.Y., Zhou, X.H., 2003. Osmium isotopic constraints on the age of lithospheric mantle beneath Northeastern China. Chemical Geology 196, 107–129.

Wu, F.Y., Yang, J.H., Zhang, Y.B., 2006. Emplacement ages of the Mesozoic granites in southeastern part of the Western Liaoning Province. Acta Petrologica Sinica 22, 315–325 (in Chinese with English abstract).

Yang, J.H., Wu, F.Y., Wilde, S.A., 2003. A review of the geodynamic setting of large-scale Late Mesozoic gold mineralization in the North China Craton: an association with lithospheric thinning. Ore Geology Reviews 23, 125–152.

Ye, H.Y., Wang, J.J., 1985. Mo-bearing pluton geological age of lower Lanjiagou of Liaoning Province. Henan Geology (Supp.) 204–205 (in Chinese with English abstract).

Yu, L.Y., 1992. The relations between granite and molybdenum deposits in Lanjiagou mining area. Mining Geology 13, 29–36 (in Chinese with English abstract).

Zhai, M.G., Xiao, W.J., Kusky, T., Santosh, M., 2007. Tectonic evolution of China and adjacent crustal fragments. Gondwana Research 12, 1–3.

Zhou, J., Griffin, W.L., Jaques, A.L., Ryan, C.G., Win, T.T., 1991. Geochemistry of diamond indicator minerals from China. Abstract, 5th International Kimberlite Conference, Brazil, pp. 475–477.

Zhou, J., Griffin, W.L., Jaques, A.L., Ryan, C.G., Win, T.T., 1994. Geochemistry of diamond indicator minerals from China. In: Meyer, H.O.A., Leonardos, O.R. (Eds.), Diamonds: Characterization, Genesis and Exploration. CPRM Special Publication, vol. 1B/93, pp. 285–301.

Zhao, G.C., Wilde, S.A., Cawood, P.A., Lu, L.Z., 1998. Thermal evolution of the Archaean basement rocks from the eastern part of the North China Craton and its bearing on tectonic setting. International Geology Review 40, 706–721.

Zhao, G.C., Cawood, P.A., Wilde, S.A., Lu, L.Z., 2000. Metamorphism of basement rocks in the Central Zone of the North China Craton: implications for Paleoproterozoic tectonic evolution. Precambrian Research 103, 55–88.

Zhao, G.C., Wilde, S.A., Cawood, P.A., Sun, M., 2001. Archean blocks and their boundaries in the North China Craton: lithological, geochemical, structural and P–T path constraints and tectonic evolution. Precambrian Research 107, 45–73.

Zhao, G.C., Sun, M., Wilde, S.A., Li, S.Z., 2005. Late Archean to Paleoproterozoic evolution of the North China Craton: key issues revisited. Precambrian Research 137, 149–172.

Zhou, X.M., Li, W.X., 2000. Origin of Late Mesozoic igneous rocks in Southeastern China: implications for lithosphere subduction and underplating of mafic magmas. Tectonophysics 326, 269–287.

Zhou, X.M., Sun, T., Shen, W.Z., Shu, L.S., Niu, Y.L., 2006. Petrogenesis of Mesozoic granitoids and volcanic rocks in South China: a response to tectonic evolution. Episodes 29, 26–33.

Zorin, Y.A., Zorina, L.D., Spiridonov, A.M., Rutshtein, I.G., 2001. Geodynamic setting of gold deposits in Eastern and Central Trans-Baikal (Chita Region, Russia). Ore Geology Reviews 17, 215–232.

Zhu, G., Wang, Y.S., Liu, G.S., Niu, M.L., Xie, C.L., Li, C.C., 2005. $^{40}Ar/^{39}Ar$ dating of strike-slip motion on the Tan-Lu fault zone, East China. Journal of Structure Geology 27, 1379–1398.